MinnesotaCorn RESEARCH & PROMOTION COUNCIL

FINAL REPORT

PROJECT TITLE: Efficient Range Extender Using E85 and Thermochemical Recuperation
PROJECT NUMBER: 1097-19EU
PRINCIPAL INVESTIGATOR: William Northrop

ABSTRACT

This research at the University of Minnesota's Thomas E. Murphy Engine Research Laboratory (UMN-MERL) enables efficient and environmentally sound utilization of ethanol blends in internal combustion engines. Future engines may play a supporting role in electrified vehicles by serving as battery charging range extender (REx) engine-generators. This project used E15 in a novel exhaust reforming strategy to increase the efficiency of spark-ignited REx engines. The proposed system utilized the waste heat from an engine to reform a portion of the incoming fuel to a fuel mixture that has higher caloric value in a process known as thermochemical recuperation (TCR). Ethanol at higher blending ratios has advantages for TCR compared to pure gasoline or E10 due to its lower catalytic steam reforming temperature, enabling higher levels of reformed fuel, thus higher engine system efficiency. The University of Minnesota developed, built, and tested a thermally integrated catalytic reactor technology during the project. The reactor utilized both the thermal energy contained in the engine exhaust and the chemical energy from oxidizing unburned fuel components from combustion to feed the reforming reaction. Experimental results showed that the reactor led to over a three percent increase in thermal efficiency due to the TCR reactor. Modeling results show that a practical implementation of the TCR system could increase engine efficiency. Greater ethanol use and use for range extension in electric vehicles benefits corn farmers by providing future market stabilization as light duty transportation moves away from fossil fuel sources.

INTRODUCTION

Vehicle electrification has accelerated as global fuel efficiency standards have become more stringent and battery costs have decreased. Although full electrification, i.e.; battery electric vehicles, may be appropriate for some light-duty vehicle applications, many vehicles will still require an engine to overcome range limitations. Range extender (REx) engine generators can be used to charge vehicle batteries as needed to meet driver demands. One advantage of REx engines is that they do not have a direct mechanical connection to the wheels and can frequently operate within the most efficient speed and load ranges. Therefore, REx engines provide an opportunity to implement advanced engine technologies that are more difficult to apply in conventional engine-powered vehicles.

Thermochemical recuperation (TCR) schemes use exhaust waste heat to catalytically convert a portion of the fuel into a gas that has increased heating value. TCR schemes may be ideal for REx engine architectures because they operate best at relatively high engine load and because they do not respond well to rapid transients. TCR may also be more beneficial than turbocharging for small engines used in REx applications because their efficiency is not dependent on thermodynamic limitations of small rotating fluid machinery.

Catalytic reforming reactions for hydrocarbon fuels include partial oxidation, steam reforming, and water gas shift as shown for octane in Equations 1-3. These are common industrially performed reactions that can be accomplished over base metal or precious metal catalysts [1]. All three reactions result in the

production of syngas, a gas consisting of hydrogen (H2) and carbon monoxide (CO). Partial oxidation is an exothermic reaction that results in net heat and lower energy content products. Steam reforming is endothermic and results in a positive chemical energy balance due to the addition of heat from an external source. The water gas shift reaction is also relevant at reforming temperatures and is generally included. Some balance of partial oxidation and steam reforming is usually desired in compact reforming since the heat from partial oxidation can be used for the steam reforming reaction.

Partial Oxidation:

$$C_8H_{18} + 4O_2 \leftrightarrow 8CO + 9H_2 \quad \left(-612.7\,\frac{kJ}{mol}\right) \qquad \text{(Eq. 1)}$$

Steam Reforming:

$$C_8H_{18} + 8H_2O \leftrightarrow 8CO + 17H_2 \quad \left(1326.5\,\frac{kJ}{mol}\right) \qquad \text{(Eq. 2)}$$

Water Gas Shift:

$$CO + H_2O \leftrightarrow CO_2 + H_2 \quad \left(-41\,\frac{kJ}{mol}\right) \qquad \text{(Eq. 3)}$$

Thermochemical recuperation through catalytic reforming processes has been studied in recent years and the progress on such systems has been reviewed [1]. Reforming processes in engines are most efficiently accomplished using both exhaust waste heat to drive reaction kinetics and using exhaust products as reactants. Methods for using exhaust gas to reform fuels include both in-cylinder, external reactors, and combinations of the two. In-cylinder reforming has been accomplished through direct injection into the negative valve overlap period of the four-stroke engine cycle [3-6]. The primary benefits of negative valve overlap reforming include its simplicity, though engine efficiency gains are small due to the low reformed fuel flow rates and poor fuel conversion to hydrogen due to short residence times.

So-called dedicated exhaust gas recirculation (EGR) concepts have been proposed that reform fuel in a single fuel-rich cylinder that feeds products back to the remaining three cylinders [7-9]. This strategy is advantageous in that it uses no catalysts to reform the fuel; however, the lack of catalyst greatly reduces reforming conversion. Others have combined dedicated EGR concepts with catalytic reactors. These systems have increased potential for TCR and have been shown to result in increased engine thermal efficiency [10-14]. Catalytic systems have an advantage in that the products from the dedicated EGR cylinder can provide the necessary heat directly to the reforming catalyst. However, controlling one cylinder separately from the others presents a control challenge. Furthermore, in previously reported dedicated EGR systems, only the waste heat from the dedicated cylinder is used to feed endothermic reforming. Heat from the remaining three cylinders is not used, thus reducing the potential to reclaim exhaust energy.

Other work has examined reforming for diesel engines where combination of partial oxidation and steam reforming are used to produce syngas [15-16]. Since syngas has lower autoignition reactivity than diesel, engine efficiency can be increased through enabling reactivity-controlled compression ignition combustion modes. However, indicated cycle efficiency gains are offset by lower energy ratios across the reforming reactor due to the reliance on partial oxidation reactions.

This project studied a novel TCR method that uses waste sensible and chemical heat from a spark-ignited REx engine to steam reform a fraction of the total incoming fuel using EGR as the steam source. Experimental results from a BMW REx engine-generator without the TCR reactor were used to validate a 1-D GT-Power model and experiments were conducted with a TCR module on a single fired cylinder. The TCR reactor was modeled, both to determine catalyst performance, and integrated with the baseline engine model. A parametric modeling study was conducted over a range of EGR rate at the highest efficiency operating speed and load point using iso-octane as the fuel. The modeling was done to illustrate how the developed TCR scheme can be used to increase fuel conversion efficiency of spark-ignited engines used in REx applications with ethanol blends as the fuel.

OBJECTIVE AND GOAL STATEMENTS

The primary objective of this project was to determine the feasibility of using a TCR system with ethanol fuel blends to increase the efficiency of internal combustion engines to be potentially used in REx applications. Specific goals in the original work plan were as follows:

1) Characterize catalyst supplied by external supplier for steam reforming with simulated exhaust gas and different ethanol/gasoline blends using bench-scale reactor
2) Simulate two-cylinder BMW REx engine generator and thermochemical recuperation reactor with ethanol blends using 1-D engine modeling software.
3) Design and construct thermally integrated catalytic reactor for BMW REx engine.
4) Determine electrical efficiency improvements with catalytic reactor installed on BMW REx engine using ethanol/gasoline fuel blends.
5) Revise reactor as needed and disseminate findings through conference presentations, journal publications, and discussions with OEMs.

MATERIALS AND METHODS

1) **Catalyst and Reactor Characterization:** Catalyst data and a model were created to evaluate steam reforming of gasoline with ethanol blends. Numerical simulations were conducted to gain a preliminary understanding of the exhaust gas reforming process involving endothermic isooctane steam reforming over a supported Rh catalyst and exothermic oxidation of engine exhaust gas using a three-way catalyst coupled through a novel thermally integrated reactor. The developed TCR reactor utilizes both the sensible energy from the elevated exhaust gas temperature in combination with the chemical energy from oxidation of the unburnt hydrocarbons and CO in the three-way catalyst (TWC). Each annular metallic monolith section which is the oxidation catalyst brazed to a tubular support which is brazed to a cylindrical metallic monolith acting as the reforming catalyst. The reformer and the exhaust gas flow in a parallel configuration inside the reactor. The design of the reactor is selected based on the conditions which provides the maximum conversion and least pressure drop in the reactor. The reactor has been designed in a compact structure that less space and can be incorporated efficiently in the exhaust of the reformer.

   A quasi-2-D model was developed to study variation of temperature, species mole fraction, heat transferred, fuel conversion, and energy ratio of the steam reformer. Heat transfer between annular, catalyst coated metal monoliths that represent endothermic and exothermic reactor sides were modelled using a spatial resistance network. This work provides critical information to evaluate the range of operability of REGR systems for use in stoichiometric SI engines and motivates future experimental work to demonstrate a novel TCR reactor concept.

   The thermal and chemical behavior of the TCR reactor was predicted by solving the conservation of mass, energy, and species equation. The model was developed considering the assumptions of steady state, fully developed flow, constant fluid properties, uniform pressure across the monolith cross section and negligible conduction in monolith fins. The reactor assembly modeled in this work consisted of concentric catalyst units connected thermally by a shared wall. Modeling was accomplished using a discrete control-volume approach. The reactor was broken into walls and gas channel rings based on input geometry. Each channel and wall were then discretized along the axial length into equal lengths. At a given axial length, all discrete channels of catalysts are solved both chemically and thermally respectively. The resulting thermochemical properties are then passed to the next set of discrete volumes to be solved again, until the outlet axial length is reached. The model setup is illustrated in Figure 1. The boundary conditions are shown in Table 1.

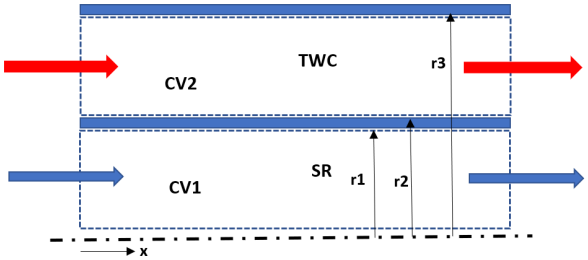

Figure 1. Model setup of the coupled reactor

Table 1. Engine conditions considered in the TCR catalyst evaluation model

	Condition 1	Condition 2	Condition 3	Condition4
Speed (rpm)	1500	1500	2000	4000
BMEP (bar)	5	9	10	15
TWC Inlet (C)	440	495	640	880
Exh Flow(kg/s)	0.014	0.0246	0.039	0.122
SR Inlet (C)	390	462	590	830
SR Flow (Kg/s)	0.0035	0.0061	0.00975	0.0305

2) **1-D Simulation:** *TCR Reactor Design:* The TCR reactor considered here is like reactors proposed by our group in prior work using ethanol as a fuel [17]. Figure 2 shows an illustration of the overall TCR engine and reactor scheme. The engine operates at a stoichiometric air to fuel ratio such that there is no excess oxygen in the exhaust gases. Like in Ref [18], a reformed EGR concept is used where vaporized fuel is added to the EGR stream prior to a reforming catalyst. Reformed EGR is advantageous because steam needed for the SR reaction does not need to be externally provided.

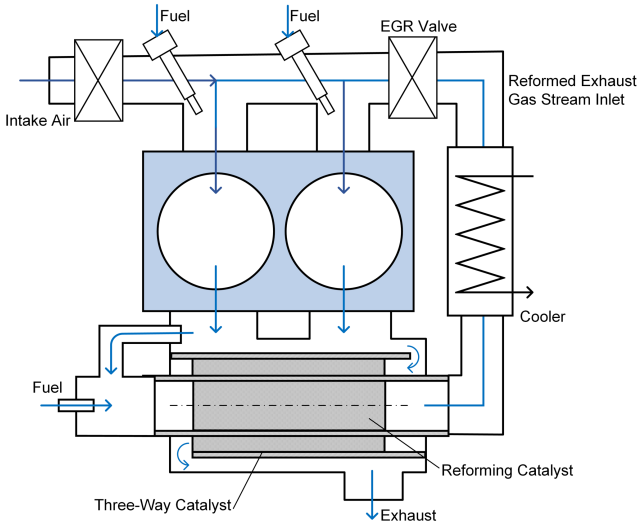

Figure 2. Illustration of the two-cylinder engine with integrated TCR reactor.

The reactor modeled in this study is unique in that it uses both the sensible (thermal) heat from the exhaust and chemical energy through oxidation of unburned hydrocarbons and CO over a three-way catalyst (TWC). The TWC and reforming catalysts are in thermal communication in the exhaust

manifold embedded in a counter-flow catalytic heat exchanger arrangement. In our previous work [17], such a reactor was reduced to practice by using concentric metallic monolith catalyst substrates separated by a stainless-steel wall through which heat could be easily conducted.

After the fuel is reformed to syngas, it is sent through an EGR cooler and valve prior to being mixed with intake air. Fuel is port-injected in the engine considered, though where fuel is injected is irrelevant to the objectives of this study.

Engine Experiments: A BMW i3 REx, two-cylinder, 0.647 L, naturally aspirated engine with port-fuel injection was used in the experimental portion of this work. Table 2 details relevant engine specifications. The engine was factory coupled to a DC generator. Both the engine and the generator have controllers which communicate over a closed area network (CAN) bus. A supervisory controller was used to operate the system that controlled both engine and generator through CAN communication. A National Instruments LabVIEW program was developed to act as the supervisory controller. The program allowed control of the engine speed and generator loading and retained the stock engine calibration.

This REx engine-generator is typically interfaced with the vehicle battery operating at approximately 370 volts DC. The battery provides energy to start the engine as well and acts as a load for the generator. In this test cell application, a small 400-volt DC battery bank was installed along with a computer controlled 500 VDC 7-amp power supply to provide DC power to the system for starting and load leveling. To load the system, a resistive load bank consisting of two 11.5 Ohm high power resisters was connected to the high voltage power bus. Computer controlled contactors allowed the load bank to operate at 5.75, 11.5 or 23 ohms. A diode was placed on the output of the high voltage power supply to prevent the generator from back feeding power.

Table 2. BMW REx engine specifications

Model Number	W20K06U0
Displacement (cc)	647
Bore x Stroke (mm)	79 x 66
Compression Ratio	10.6:1
Power Output (kW)	25 @ 4300 rpm
Torque (Nm)	44 @ 4300 rpm
Induction	Naturally Aspirated
Valves per cylinder	4
Exhaust emissions legislation	SULEV II

External fuel and water-cooling systems were installed to mimic vehicle operation and additional temperature and pressure sensors were installed to ensure safe test cell operation. Fuel flow was measured using a day tank and programmable scale. Gaseous emissions were measured using an AVL SEASAM i60 Fourier Transform Infrared emissions bench for a subset of the operating points. In the testing, 34 engine speeds and loads were tested to determine the engine efficiency map and five steady state speed and load conditions were run to validate the 1-D GT-Power model. These modes are shown in Table 3 and were selected to cover the range of peak engine operating efficiency.

Table 3. Engine speed and electric load conditions tested in the experiments used to validate the 1-D engine model.

Case	Speed (rpm)	Electric Power (kW)
1	2700	11.1
2	3000	5.1
3	3000	10.7
4	3300	13.5
5	3300	11.8

1-D Engine and TCR Model: A model of the 2-cylinder BMW REx engine was built in the GT-Power 1-D simulation environment. It was comprised primarily of an engine model and an integrated aftertreatment model. The flowsheets of both models are given in the Appendix. The engine model used intake and exhaust and cylinder geometry measured from the test engine described in the previous section. The model without the TCR reactor was run using the default combustion model provided in GT-Power. This baseline model did incorporate the close-coupled TWC that is used in the vehicle and provided with the REx engine. Throttle valve open percentage and backpressure were tuned for each of the conditions given in Table 2 at the given engine speeds to achieve the same brake output power as was found in the experiments. Brake power output from the experiments was calculated assuming 90% generator efficiency.

The engine was operated with a stoichiometric air to fuel ratio for all the modeling and experiments. This mixture was maintained by controlling the oxygen concentration in the exhaust manifold to a constant value determined from experimental measurements. The engine fuel to air ratio was not specified in the model due to the need to account for gaseous fuel contained in the reformed EGR stream. Therefore, a controller was inserted into the model to control fuel injected to match a desired exhaust O2 concentration. The fuel used in the modeling was pure iso-octane though non-oxygenated pump gasoline (90 RON) was used in the experimental work. The engine combustion model for all simulations was a Wiebe Function with an assumed a constant combustion phasing of 50% mass fraction burned crank angle (CA50) of 7.0 degrees after top dead center. The combustion duration did not change with fuel type and the combustion efficiency was maintained at 97%.

A conceptual diagram of the counter-flow TCR model is shown in Figure 3. In the model, the exhaust gas and EGR stream are in a counter-flow configuration. Each catalyst section was assumed to consist of a 100 cells per square inch monolith substrate. The three-way catalyst was assumed to have a total volume of 2.0 liters and the reforming catalyst had a volume of 1.0 liters. Heat was transferred between sections by assuming a conductive metal path between them.

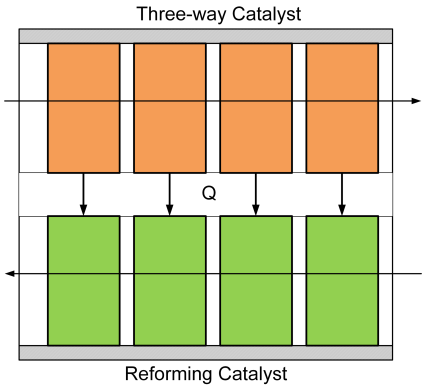

Figure 3. Conceptual model of the opposed flow reactor model built in GT-Power for the 1-D simulations. Two monolithic catalyst sections interacted through a thermal boundary to exchange both chemical and sensible heat.

The baseline chemical kinetic model for the TWC reactor provided in a template in GT-Power was used. Limited literature exists describing the kinetics of gasoline steam reforming. Steam reforming kinetics for iso-octane over nickel catalysts provided by Praharso et al. [19] were used for the reforming section. Only steam reforming (Eq. 1) was assumed to occur. However, dry reforming and some partial oxidation from residual carbon dioxide and oxygen in the engine exhaust, respectively would most likely also occur in an actual reactor.

3) **Engine and TCR Reactor:** A thermally integrated reforming reactor shown in Figure 4, was designed and fabricated for use the research project. A 500 W vaporizer was used to inject fuel vapor into the reforming section. The engine used in this study was BMW N43B20 gasoline direct injection (GDI) engine. Specification of the engine are listed in Table 4. The engine was run on a single cylinder while the other cylinders were motored. Exhaust species concentrations were measured using Fourier-Transform Infrared (FTIR) spectroscopy. Reformer species concentration were measured using Nova gas analyzer and other engine parameters were measured using K-type thermocouples and pressure transducers. The engine and reactor operating conditions were varied to examine system performance under different variables. The total fuel flow rate going to the reactor and engine was kept constant and the IMEP was allowed to vary for each EGR conditions. AVL GH14D pressure sensors and AVL INDICOM system were used to record the in-cylinder pressures and IMEP calculations. The diagram of the engine test setup is shown in Figure 5.

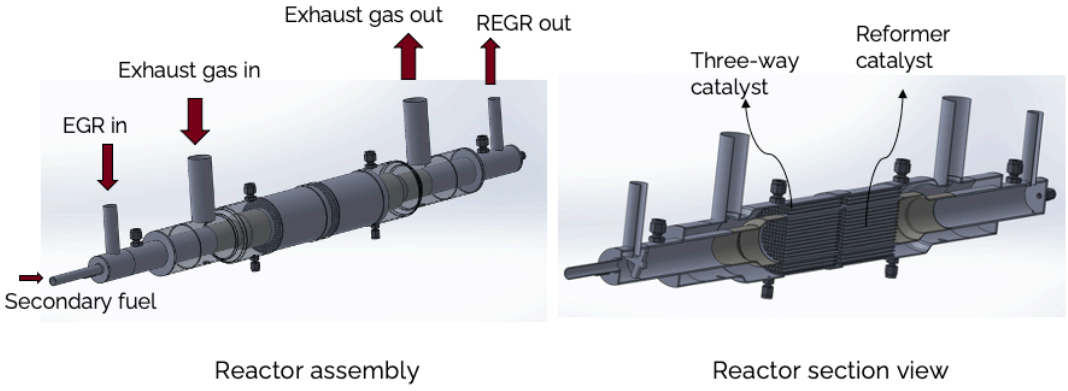

Figure 4. Illustration of the experimentally evaluated TCR reactor including a cutaway (left panel) showing catalyst locations.

Table 4: Specifications of engine used in TCR reactor experiments

Model Number	N43B20
Displacement (cc)	1995
Bore x Stroke (mm)	84 x 90
Compression Ratio	12:1
Rated Power (kW)	125 @ 6700 rpm
Rated Torque (Nm)	210 @ 4250 rpm
Induction	Naturally Aspirated
Injection	Central Spray Guided Piezo
Max Rail Pressure (bar)	200

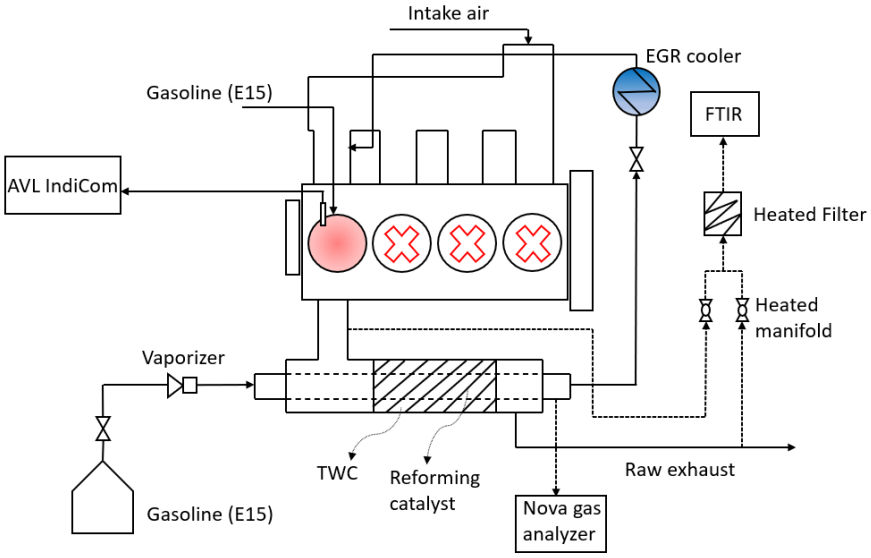

Figure 5. Setup of single cylinder gasoline engine used for the TCR experiments.

RESULTS AND DISCUSSION

1) **Characterization of TCR Catalyst and Reactor:** In the endothermic reforming side of the reactor, thermal energy from the engine exhaust and exothermic reaction from the TWC drives the reaction. The model results show a gradual temperature rise in the entrance as seen in Figure 6 (a-b). For the case of 2000 rpm and 4000 rpm engine speed, the inlet temperature of the gases in the reformer is 863 K and 1103 K, which is sufficiently high to accelerate the steam reforming reaction. But initially there is less heat transferred from the TWC exothermic side leading to drop in temperature in the center of the reformer away from the interface. The average temperature decreases during this period. However, diffusion of heat increases along the along length which acts as a driving force for the endothermic reaction leading to temperature rise at outlet of the steam reformer.

At the entrance of the steam reformer, the inlet temperature for engine condition 3 is lower than that of engine condition 4 which affects the reaction rate and thus the initial production of hydrogen. However, with the rise in reformer temperature H_2 increases significantly along the length. Hydrogen concentration as high as 0.134469 mole fraction was observed. The energy ratio is defined to find the degree of increase of heating value of the original fuel. It can be defined as the ratio of lower heating value of the syngas to the lower heating value of original fuel as in Equation 4.

$$\eta_{reformer} = \frac{LHV(H2)\times FH2+LHV(CO)\times FCO+LHV(C8H18)\times FC8H18}{LHVC8H18\times FC8H18|x=0} \quad \text{(Eq. 4)}$$

With rise in engine exhaust temperature, the reformer energy ratio increases as shown in Figure 7. This is because with higher exhaust temperature and higher exhaust mass flow rates, the temperature in the TWC increases which favors higher heat transfer to the SR reactor. This leads to increase in concentration of hydrogen and carbon monoxide thereby facilitating rise in reformer energy ratio. The rise in reactor temperature also favors higher fuel conversion.

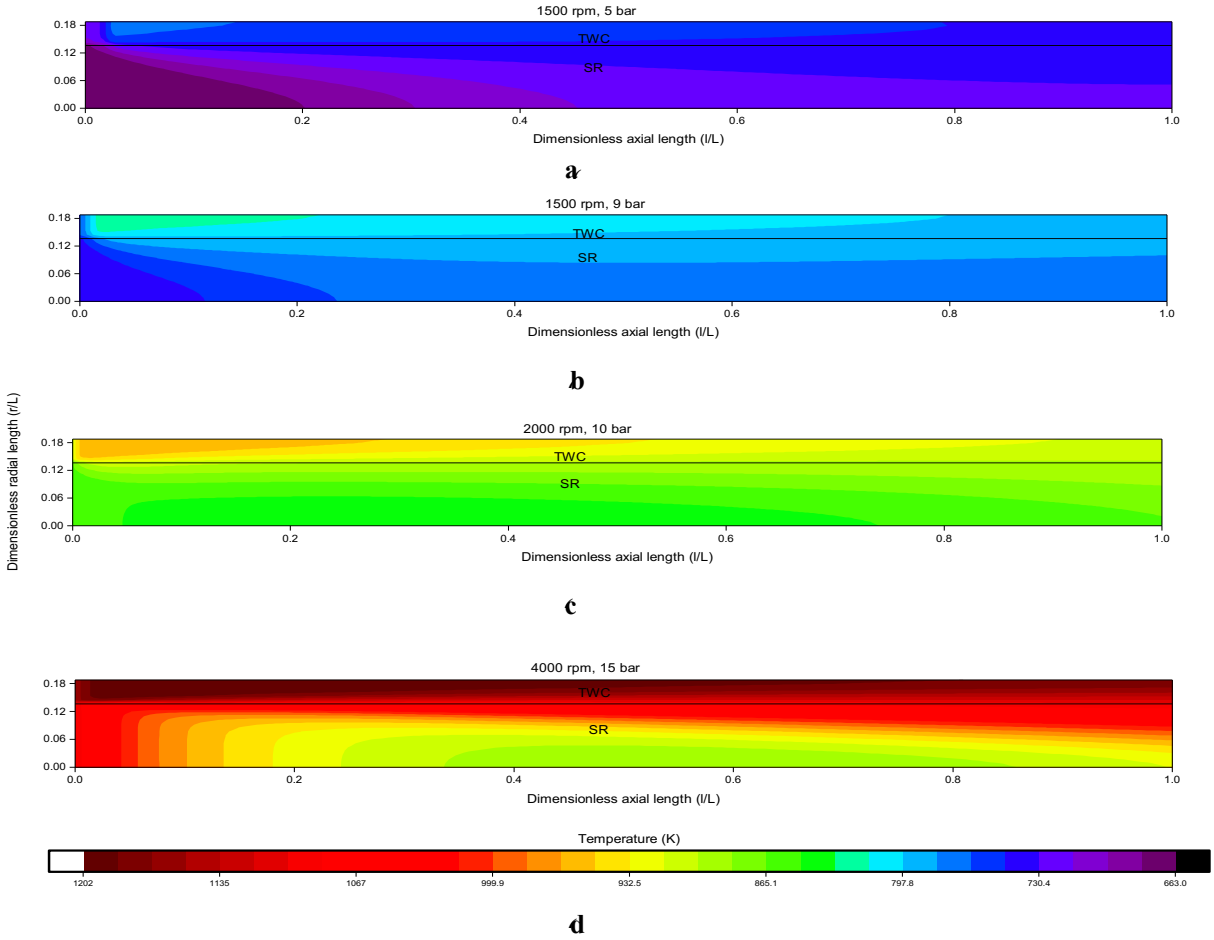

Figure 6. Temperature distribution for (a) 1500 rpm, 5 bar engine condition, T_e = 713 K (b) 1500 rpm, 9 bar engine condition, T_e = 768 K (c) 2000 rpm, 10 bar engine condition, T_e = 923 K (d) 4000 rpm, 15 bar engine condition, T_e = 1153 K.

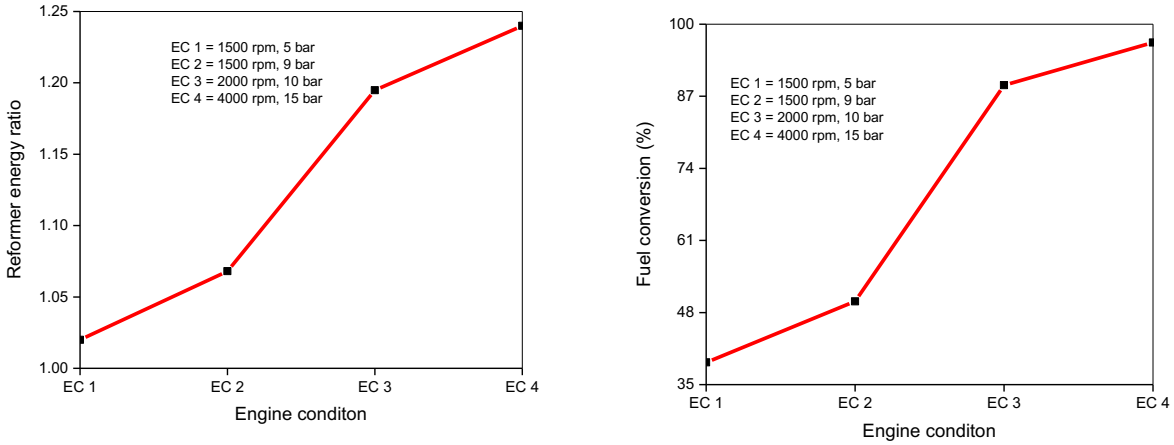

Figure 7. Reformer energy ratio variation with engine conditions

With higher load and higher exhaust temperature the pressure drop in the oxidation catalyst increases significantly and it is detrimental to the reactor design. The feasibility of coupling is verified as there is a 18% to 25% increase in the heating value of the REGR.

2) **1-D REx Engine Model:** *Engine Performance and Model Validation:* The efficiency map from engine experiments conducted over 34 speed and load conditions is shown in Figure 8. The specific fuel consumption is reported based on the electric power output and is shown as electric specific fuel consumption (ESFC). The wide-open throttle (WOT) power curve was not experimentally found and therefore, the peak power for a given engine speed was not determined. Regardless, the figure shows that the highest efficiency island for the engine conditions tested resides at 2700 rpm engine speed. Therefore, this speed at the highest load of 11.1 kWe was selected for studying the TCR reactor (Case 1) in Table 2.

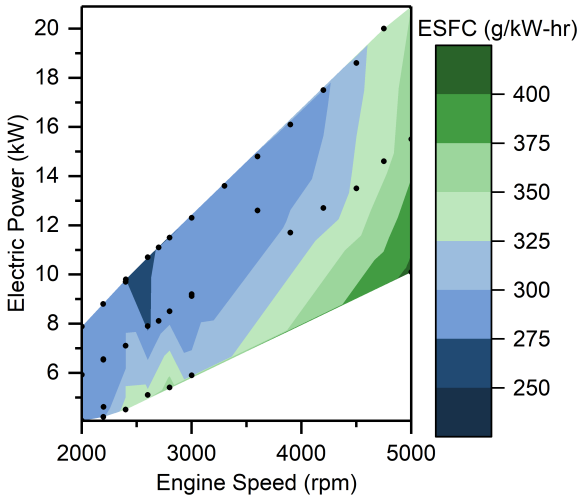

Figure 8. BMW 2-cylinder REx engine electric-output specific fuel consumption as measured in the laboratory testing.

The baseline engine model without the TCR reactor was validated at five of the 34 engine operating conditions given in Table 1. Results of the validation work for each condition is given in Table 5. In the table, the corresponding BMEP for each case and the measured BSFC and exit O_2 concentration is provided. The baseline model was also validated for other emissions values, but since these are not central to the discussion in this paper, they are omitted for brevity.

Table 5. Validated baseline model BSFC and engine-out O2 concentration data. "Exp" is experimental data, "Mod" is the modeled data, and "Err" is the percentage error between the experimental and model data given in percent. Case 1 (bold) was chosen as the best BSFC condition for further study with the TCR reactor model.

Case	Speed (rpm)	BMEP (bar)	BSFC (g/kWhr)	Engine-Out O_2 (ppm)				
			Exp	Mod	Err	Exp	Mod	Err
1	**2700**	**8.4**	**252**	**240**	**5%**	**5008**	**5022**	**0.3%**
2	3000	3.2	341	346	1%	6026	6077	0.8%
3	3000	6.6	282	278	2%	5348	5401	1.0%
4	3300	6.6	285	281	1%	4571	4616	1.0%
5	3300	7.6	284	276	3%	4121	4160	0.9%

Integrated TCR Reactor Performance and Emissions Simulation: The integrated model was run holding the throttle position and engine speed constant. Therefore, the BMEP of the engine dropped as the EGR percentage increased. As stated earlier, with increasing EGR percentage, the percentage of fuel sent to the reformer section versus the engine increased because the molar steam to carbon

ratio (S/C) was held constant at 1.0. All plots shown in this section depict performance over the range of EGR run in the parametric study from 0-32%.

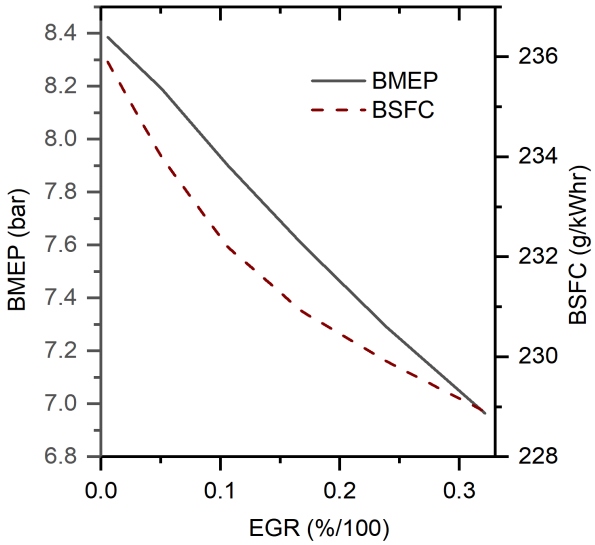

Figure 9. BMEP and BSFC as a function of EGR.

Figure 9 provides the BMEP and BSFC of the engine versus EGR percentage. While the BMEP decreased by 1.4 bar with increasing EGR, the BSFC improved by 2.9% through the use of the TCR reactor. The manifold inlet pressure also increased by 4 kPa (not shown) over the EGR range. To increase engine load for higher EGR rates, enough pressure difference must exist between the exhaust and intake manifold, which will ultimately restrict the maximum load for a TCR equipped engine. However, for REx engines, the engine need not operate at WOT since there is no vehicle acceleration requirement. Therefore, an engine could be designed to operate with sufficient pressure differential to drive EGR at one peak efficiency point.

Figure 10 shows the overall performance of the reforming reactor at the chosen operating point. The fuel fraction sent to the reformer over the total fuel sent to the engine and reformer increased from zero with no EGR to up to approximately 50% at the highest EGR point. However, the fuel conversion through the reformer, defined as the percentage of fuel converted to H2 and CO also decreased with increasing EGR due to insufficient residence time in the catalyst. The peak gas hourly space velocity based on standard conditions (298 K and 101 kPa) at the highest EGR rate was 10,556 hr-1. For the Ni-based SR catalyst described in [19], such a short residence time is only capable of converting about 22% of the fuel. If a larger reforming catalyst is used, or one with precious metal active materials, as was used in our previous experimental work for hydrous ethanol [17], it is expected that even greater conversion could be achieved at higher EGR rates. The energy ratio, defined as the lower heating value of reforming products to that of the reactants into the reactor was highest with the highest conversion. Therefore, if the conversion could be increased at higher EGR rates, the energy ratio would increase and the engine BSFC could be further improved. More experimental data from actual reforming reactors are necessary to determine SR kinetics at engine relevant conditions and with appropriate substrates before true efficiency improvement potential of the TCR reactor can be predicted.

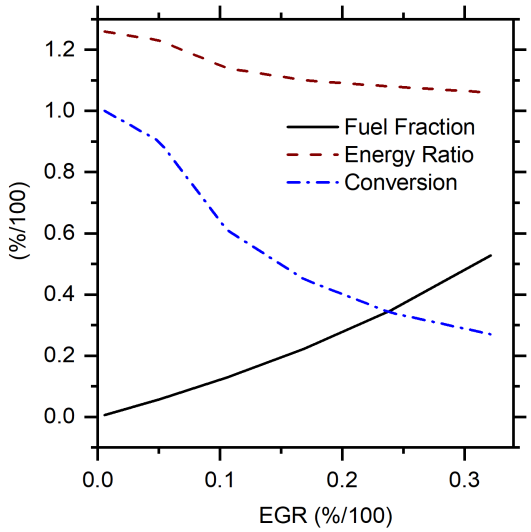

Figure 10. Reformer fuel fraction, reformer total energy ratio, and reformer catalyst conversion efficiency as a function of EGR.

The TCR reactor operates by converting both sensible heat from the exhaust with chemical energy from the TWC oxidation reactions to increase SR reaction conversion efficiency. The 2.9% decrease in BSFC of the engine shown in Figure 9 is a result of heating value improvement of the reformed fuel (i.e.; positive energy ratio) in proportion to the quantity of fuel reformed. Therefore, even though the energy ratio was the highest for low EGR, the amount of fuel reformed was near zero, so the net fuel efficiency benefits were lower. However, although the energy ratio for high EGR was only slightly above one, over 50% of the fuel to the engine, times 25% conversion, or 12.5% of the total fuel was converted to products with higher energy content.

Figure 11 illustrates the temperatures into and out of the TWC reactor as depicted in Figure 2 as a function of EGR rate. As the EGR rate increased, the TWC inlet temperature (i.e., engine exhaust manifold temperature) decreased by over 100 °C. This decrease in temperature is also responsible for the decrease in reformer fuel conversion shown in Figure 5, along with increasing GHSV. The difference in temperature between the TWC inlet and the reformer inlet is due to the lower temperature (400 K) fuel vapor mixing before the EGR stream enters the TCR reactor. As previously stated, the latent heat of vaporization for the iso-octane is not considered in the model.

Overall, significant heat is extracted through the TWC reactor as the fuel fraction to the TCR reactor increases. Heat loss to the ambient is also responsible for reduced temperature through the TWC and reformer. The outlet temperature of the reformer is reduced to approximately 550 °C at the highest EGR rate, a marginal temperature for SR kinetics over Ni or precious metal catalysts. In general, higher exhaust temperature is desired for allowing greater reformer conversion. For REx applications, it may be desired to consider semi-adiabatic engine modifications like ceramic coatings on in-cylinder surfaces to increase exhaust enthalpy compared to heat leaving the engine system through the coolant.

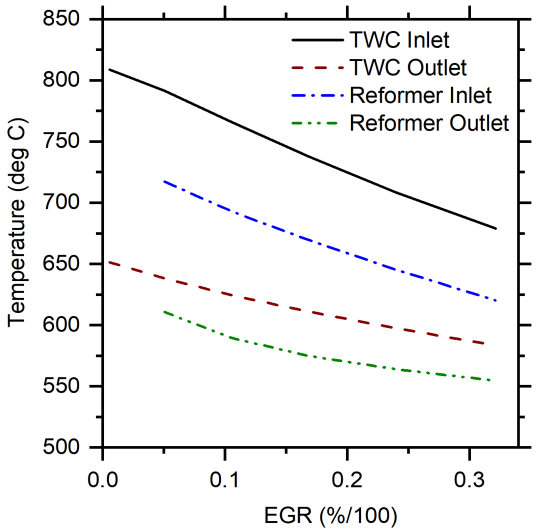

Figure 11. Temperatures in and out of the TCR reactor on both the TWC side and the reformer side as a function of EGR.

Figures 12 and 13 provide the mole fraction predictions of iso-octane fuel and reforming products, H_2 and CO at the exit of the reforming reactor and in the engine intake manifold (prior to fuel injection), respectively. At zero EGR, the H_2 and CO mole fractions in the reformer exit necessarily go to zero, a discontinuity in the modeling results not shown in the figures. The peak mole fraction of H_2 achievable in the products is approximately 22%, though this decreased with EGR rate due to the decreasing fuel conversion through the reforming reactor as shown previously.

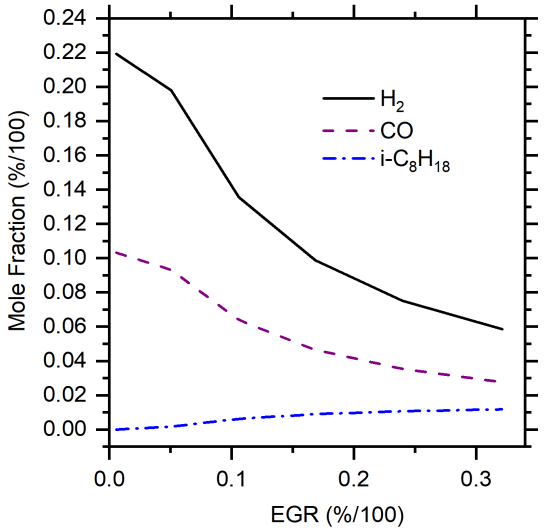

Figure 12. Reforming catalyst mole fractions of H2, CO and iso-octane as a function of EGR.

At the highest EGR setting the peak H2 mole fraction in the intake approached 1.6%. Literature evidence shows that even with such low concentrations of H2 in the intake air, improvements in spark-ignition engine performance can be achieved. For example, Ji et al. [20] showed in a modeling study that 2% H_2 in the intake was ideal for maximizing indicated thermal efficiency by achieving a proper balance between combustion phasing and heat loss. Higher H_2 concentrations

led to short combustion durations that increased heat loss from excessive peak cylinder pressures and resulted in higher than desired combustion noise.

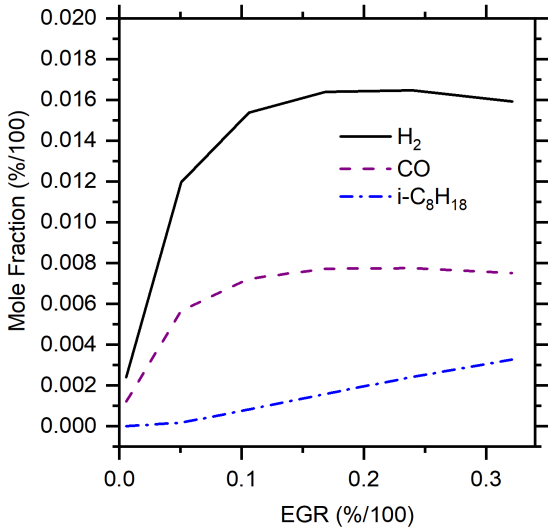

Figure 13. Engine intake manifold mole fractions of H_2, CO and iso-octane as a function of EGR.

3) **Integrated TCR and Engine Experiments:** The engine equipped with the thermally integrated reformer was operated over a range of EGR rates with splash blended E15 fuel. Results from one operating condition at 2000 rpm and 6.5 bar indicated mean effective pressure (IMEP) are reported here, though other operating conditions were tested using the engine. At that chosen operating condition, the integrated reformer achieved an energy ratio, or fumigant energy fraction (FEF) of 33.3 % as shown in Figure 14 over a range of EGR rate from 6% to just over 11%. The fuel flow rate was maintained constant through the experiments both to the TCR reactor and the engine. the figure also illustrates that the energy ratio remained above 1.0 over the course of experiments, indicating that the steam reforming catalyst converted a significant portion of the incoming E15 to hydrogen prior to the intake manifold.

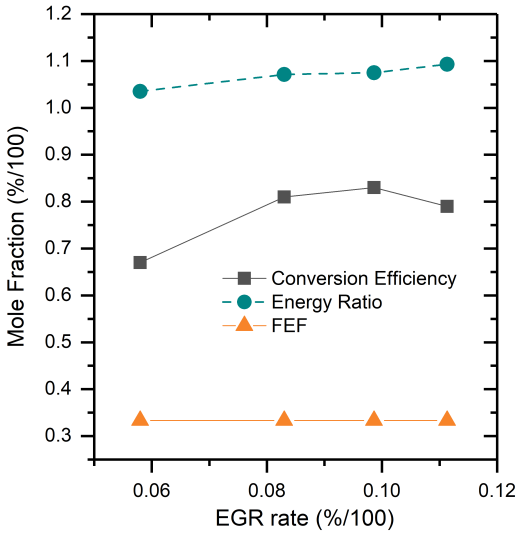

Figure 14. TCR reactor conversion efficiency, energy ratio, and fumigant energy fraction for the 2000 rpm 6.5 bar IMEP condition and E15 fuel.

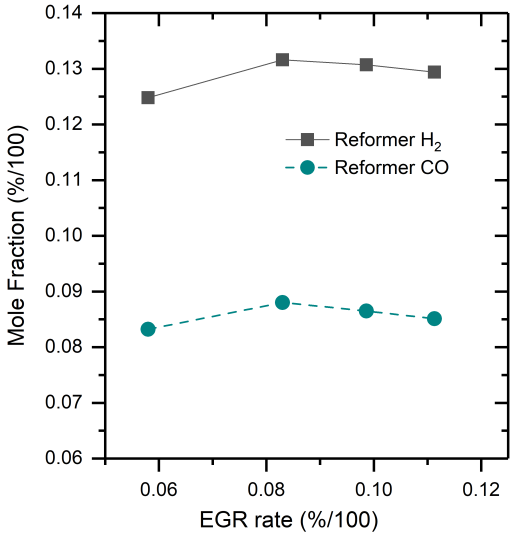

Figure 15. TCR Reactor H_2 and CO mole fractions at the catalyst exit.

Figure 15 illustrates the production of hydrogen and CO in the TCR reactor as a function of EGR rate. Both reforming products remain constant over the EGR range yet are lower than expected at the same EGR rate from the modeling results. Figure 16 shows that engine power and efficiency increased using the TCR reactor running on E15 fuel. Indicated specific fuel consumption (ISFC) is a measure of the amount of fuel burned per kW-hr. It decreased to a minimum (maximum efficiency) point at around 8% EGR rate, increasing the efficiency from the baseline case without the TCR reactor by 3%. Such an efficiency gain is significant in highly efficient modern engines.

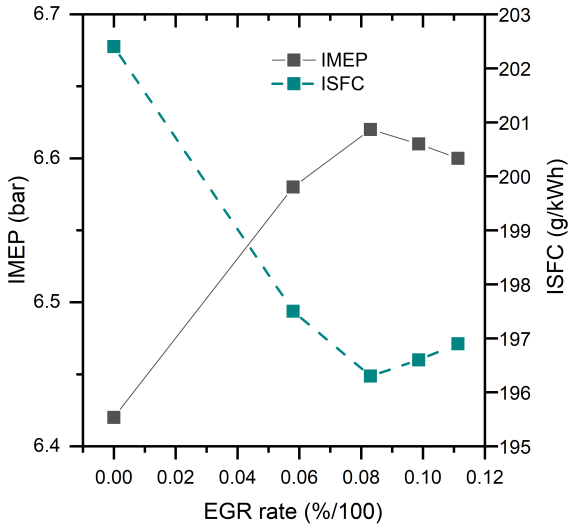

Figure 16. Indicated specific fuel consumption (ISFC) and indicated mean effective pressure (IMEP) over a range of EGR rates at 2500 rpm, 6.5 bar IMEP and E15 fuel.

CONCLUSIONS

This project showed through computer modeling and simulations that TCR using ethanol blends is a viable way to increase the efficiency of spark-ignited engines. Engines running at limited operating points are an efficient way to extend the range of electric vehicles. Since the TCR reactor operates better at constant speed and load conditions, it is an ideal technology for use in REx applications. Future work will

look to implement ethanol REx engines in electric vehicle demonstrations. Other work will look to higher blends of ethanol and hydrous ethanol as fuels for spark-ignition engines using TCR reactors. Greater ethanol use and use for range extension in electric vehicles benefits corn farmers by providing future market stabilization as light duty transportation moves away from fossil fuel sources.

EDUCATION, OUTREACH, AND PUBLICATIONS

The results of the modeling portion of the project were presented at the SAE IC Engines 2019 conference on September 16-19 of 2019, and was accepted as a journal paper by SAE. The paper is available upon request. Additional papers are expected to be published on the data shown in this report in coming years, as the data are further analyzed. The project, like previous research efforts at the Thomas E. Murphy Engine Research Laboratory (MERL) directed by the Dr. Northrop supported a Ph.D. student and an undergraduate research assistant. It provided invaluable experience for these students, not only by learning the theoretical aspects of engine modeling and experimentation, but also to generate new ideas regarding the expanded use of ethanol in engine applications. The PI Northrop and his students also regularly participated in the AG Expo, MNCGA events and other direct outreach activities to inform farmers about the research activities at the MERL.

REFERENCES

1. Aasberg-Petersen, K., Bak Hansen, J.H., Christensen, T.S., Dybkjaer, I., Christensen, P.S., Stub Nielsen, C., Winter Madsen, S.E.L., and Rostrup-Nielsen, J.R. "Technologies for Large-Scale Gas Conversion." Applied Catalysis A: General 221 (1–2), 2001, pp. 379–87. doi:10.1016/S0926-860X(01)00811-0.
2. Tartakovsky, L., and Sheintuch, M. "Fuel Reforming in Internal Combustion Engines." Progress in Energy and Combustion Science 67, 2018, pp. 88-114. doi: 10.1016/j.pecs.2018.02.003.
3. Ekoto, I., Peterson, B., Szybist, J., and Northrop, W. "Analysis of Thermal and Chemical Effects on Negative Valve Overlap Period Energy Recovery for Low-Temperature Gasoline Combustion." SAE International Journal of Engines 8 (5), 2015, pp. 2015-24–2451. doi:10.4271/2015-24-2451.
4. Cao, L., Zhao, H., and Jiang, X. "Investigation into Controlled Auto-Ignition Combustion in a GDI Engine with Single and Split Fuel Injections" 2007 (724), 2007, pp. 776–90. doi:10.4271/2007-01-0211.
5. Urushihara, T., Hiraya, K., Kakuhou, A., and Itoh, T. "Expansion of HCCI Operating Region by the Combination of Direct Fuel Injection, Negative Valve Overlap and Internal Fuel Reformation." SAE Transactions 112, 2003, pp. 1092–1100. doi:10.4271/2003-01-0749.
6. Szybist, J.P., Steeper, R.R., Splitter, D., Kalaskar, V.B., Pihl, J., and Daw, C. "Negative Valve Overlap Reforming Chemistry in Low-Oxygen Environments." SAE International Journal of Engines 7 (1), 2014, pp. 418–33. doi:10.4271/2014-01-1188.
7. Chadwell, C., Alger, T., Zuehl, J., and Gukelberger, R. "A Demonstration of Dedicated EGR on a 2.0 L GDI Engine." SAE International Journal of Engines 7 (1), 2014, pp. 2014-01–1190. doi:10.4271/2014-01-1190.
8. Lee, S., Ozaki, K., Iida, N., and Sako, T. "A Potentiality of Dedicated EGR in SI Engines Fueled by Natural Gas for Improving Thermal Efficiency and Reducing NO x Emission." SAE International Journal of Engines 8 (1), 2014, pp. 2014-32–0108. doi:10.4271/2014-32-0108.
9. Kalaskar, V.B., Gukelberger, R., Denton, B., and Briggs, T. "The Impact of Engine Operating Conditions on Reformate Production in a D-EGR Engine," 2017. doi:10.4271/2017-01-0684.
10. Randolph, Eric, Raphael Gukelberger, Terrence Alger, Thomas Briggs, Christopher Chadwell, and Antonio Bosquez Jr. "Methanol Fuel Testing on Port Fuel Injected Internal-Only EGR, HPL-EGR and D-EGR ® Engine Configurations." *SAE Int. J. Fuels Lubr.* 10, no. 3 (2017): 718–27. doi:10.4271/2017-01-2285.
11. Chang, Yan, James P Szybist, Josh A Pihl, and D William Brookshear. "Catalytic Exhaust Gas Recirculation-Loop Reforming for High." *Energy & Fuels* 32 (2018): 2257–66. doi:10.1021/acs.energyfuels.7b02565.

12. Szybist, James P, Josh Pihl, Shean Huff, Brian Kaul, and Oak Ridge. “High Load Expansion of Catalytic EGR-Loop Reforming under Stoichiometric Conditions for Increased Efficiency in Spark Ignition Engines.” *SAE Technical Paper 2019-01-0244*, 2019, 1–13. doi:10.4271/2019-01-0244.Abstract.
13. Voice, Alexander K, and Vincent Costanzo. “Fuel and Engine Effects on Rich-Combustion Products as an Enabler of In-Cylinder Reforming.” *SAE Technical Paper 2019-01-1144*, 2019, 1–18. doi:10.4271/2019-01-1144.Abstract.
14. Brookshear, D William, Josh A Pihl, and James P Szybist. “Catalytic Steam and Partial Oxidation Reforming of Liquid Fuels for Application in Improving the Efficiency of Internal Combustion Engines.” *Energy and Fuels* 32 (2018): 2267–81. doi:10.1021/acs.energyfuels.7b02576.
15. Chuahy, Flavio D F, and Sage L. Kokjohn. “High Efficiency Dual-Fuel Combustion through Thermochemical Recovery and Diesel Reforming.” *Applied Energy* 195 (2017): 503–22. doi:10.1016/j.apenergy.2017.03.078.
16. Hwang, J., Li, X., and Northrop, W. “Exploration of Dual Fuel Diesel Engine Operation with On-Board Fuel Reforming.” *SAE Technical Paper*, 2017. doi:10.4271/2017-01-0757.
17. Hwang, Jeffrey T., Kane, S.P, and Northrop, W.F. “Hydrous Ethanol Steam Reforming and Thermochemical Recuperation to Improve Dual-Fuel Diesel Engine Emissions and Efficiency.” In *Proceedings of the ASME 2018 Internal Combustion Engine Division Fall Technical Conference*, Vol. ICEF2018-9, 2018.
18. Lau, C.S., Allen, D., Tsolakis, A., Golunski, S.E., and Wyszynski, M.L. “Biogas Upgrade to Syngas through Thermochemical Recovery Using Exhaust Gas Reforming.” Biomass and Bioenergy 40. Elsevier Ltd, 2012, pp. 86–95. doi:10.1016/j.biombioe.2012.02.004.
19. Adesina, A.A, D.L. Trimm, and N. W. Cant. “Kinetic Study of Iso -Octane Steam Reforming over a Nickel-Based Catalyst.” *Chemical Engineering Journal* 99 (2004): 131–36. doi:10.1016/j.cej.2003.10.002.
20. Ji, Changwei, Hao Yan, and Shuofeng Wang. “Simulation Study on Combustion Characteristics of a Spark Ignition Engine Fueled with Gasoline – Hydrogen Fuel Mixture.” *SAE Technical Paper 2009-24-0093*, 2009. doi:10.4271/2009-24-0093